Available online at www.sciencedirect.com
SCIENCE DIRECT®
Journal of Solid State Chemistry 177 (2004) 4546–4551
JOURNAL OF SOLID STATE CHEMISTRY
www.elsevier.com/locate/jssc

A chemical route for the synthesis of cubic bismuth zinc niobate pyrochlore nanopowders

S.M. Zanetti*, S.A. da Silva, G.P. Thim

Departamento de Química, Instituto Tecnológico de Aeronáutica, Centro Técnico Aeroespacial, Pça. Marechal Eduardo Gomes, 50, Vila das Acácias, 12298-900, São José dos Campos-SP, Brazil

Received 18 March 2004; received in revised form 31 August 2004; accepted 2 September 2004
Available online 11 November 2004

Abstract

Cubic bismuth zinc niobate pyrochlore (base composition $(Bi_{1.5}Zn_{0.5})(Zn_{0.5}Nb_{1.5})O_7$) powders were successfully prepared by a chemical method. The formation mechanism of the pyrochlore phase was investigated by TG-DSC, FT-IR, Raman, and X-ray diffraction (XRD). The optical bandgap for the powders treated at temperatures ranging from 500 to 700 °C is 3.0–3.1 eV, indicating low crystallization temperature for the pyrochlore phase. No detectable intermediary phases as $BiNbO_4$ or a pseudo-orthorhombic pyrochlore were observed at any time and the cubic-BZN phase was already formed after thermal treatment at temperatures as low as 500 °C. The phase formation study reveals that a well-crystallized single-phased nanopowder is obtained after calcination at 700 °C, indicating that the chemical synthesis conferred a higher chemical homogeneity and reactivity on the powder, modifying the crystallization mechanism.

Keywords: Bi_2O_3–ZnO–Nb_2O_5; Cubic bismuth zinc niobate; Pyrochlore; Nanopowders; Chemical method; Pechini

1. Introduction

Pyrochlore and pyrochlore-related compounds in the Bi_2O_3–ZnO–Nb_2O_5 system exhibit high dielectric constants (ε), relatively low dielectric losses, and compositionally adjustable temperature coefficients of capacitance (TCC). These properties, allied to low sintering temperatures (less than 950 °C), make these compounds attractive candidates for capacitor and high-frequency filter applications in multilayer structures co-fired with metal electrodes [1].

Stoichiometric pyrochlores, whose general formula is $A_2B_2O_7$, have a structure composed of two different types of cation coordination polyhedra, in which the *A*-site positions typically occupied by larger cations are octacoordinate, while the *B*-site positions favored by smaller sized cations are hexacoordinate [2]. Their structural formula is often written as $B_2O_6 \cdot A_2O'$, which emphasizes that the arrangement consists of a three-dimensional network of octahedra (B_2O_6) linked with an A_2O' tetrahedra in the interstices.

The two basic phases of the BZN system are the cubic-pyrochlore-structure α-phase (base composition $(Bi_{1.5}Zn_{0.5})(Zn_{0.5}Nb_{1.5})O_7$) and the low-symmetry-structure β-phase (base composition $(Bi_2(Zn_{1/3}Nb_{2/3})_2O_7$). The electrical properties of the two phases are quite dissimilar (TCC ~ -400 ppm/°C for the α-phase, and TCC ~ -200 ppm/°C for the β-phase), which is an attractive feature in the manufacture of devices with controllable temperature coefficients of capacitance.

BZN-based dielectric ceramics have been systematically prepared by the conventional powder processing method and their powders and ceramics have been exhaustively studied [3–7]. It is known that the solid-state reaction method can lead to local chemical heterogeneity and large sized particles, which may result in multiphase powders.

*Corresponding author. Fax: +55-12-3947-5958.
E-mail address: zanetti@ief.ita.br (S.M. Zanetti).

0022-4596/$ - see front matter © 2004 Elsevier Inc. All rights reserved.
doi:10.1016/j.jssc.2004.09.001

One of the main applications of the BZN pyrochlore system is in the production of low-fire high-frequency multilayer capacitors with internal silver electrodes. Therefore, the interaction between silver and bismuth-based ceramics is a matter of concern for researchers. Nino et al. [4] stated that phase purity is essential for BZN compatibility with silver electrodes.

Chemical methods have offered an alternative to produce smaller sized, chemically homogeneous particles. The use of solution-based chemical methods to prepare nanocrystalline materials is expected to result in chemically homogeneous and phase-pure specimens, a narrow particles size distribution, and low crystallization and sintering temperatures of the materials.

The main purpose of this work was to obtain chemically homogeneous cubic-BZN nanopowder, to which end the polymeric precursor method was employed. The polymeric precursor is a chemical method based on the Pechini process [8] and has been successfully used to synthesize several complex oxides [9–12].

2. Experimental details

2.1. Synthesis

The α-BZN composition was synthesized by the polymeric precursor method, which consists of chelating metallic cations with citric acid, followed by polymerization through the addition of ethylene glycol. The starting reagents were bismuth oxide, Bi_2O_3 (99.99%, Aldrich), zinc acetate dihydrate, $(CH_3CO_2)_2Zn \cdot 2H_2O$ (99.5%, Carlo Erba), and niobium ammonium oxalate, $NH_4H_2[NbO–(C_2O_4)_3] \cdot 3H_2O$ (99.5%, CBMM, Araxá, Brazil). The first step involved dissolving niobium ammonium oxalate in water and precipitating $Nb(OH)_5$ by adding NH_4OH. After filtration, the niobium hydroxide was dissolved in an aqueous solution of citric acid (CA) to form niobium citrate (molar ratio CA/Nb = 3). The Nb content was gravimetrically determined as Nb_2O_5. Stoichiometric amounts of zinc acetate dihydrate as salt (0.711 g, 0.317 mmol) and Bi_2O_3 (1.11 g, 0.476 mmol), dissolved in an aqueous nitric acid solution (50 v/v%, 8 cm^3), were added to the niobium citrate solution (0.476 mmol) heated at 60 °C to form a (Zn, Nb, Bi) complex precursor. Citric acid was added to maintain the molar ratio CA/metal = 3). The solution was kept under stirring at 60 °C and the pH was adjusted to 8–9 with ethylenediamine, resulting in a clear pale yellow solution. Ethylene glycol (5.34 g) was added to this solution to promote polymerization of the mixed citrate. In this synthesis, the citric acid/ethylene glycol ratio (CA/EG, mass ratio) was 60/40.

The resin was kept on a hot plate until a viscous gel was obtained, which was then thermally treated at 300 °C for 4 h in a furnace. The powder thus obtained was treated at temperatures ranging from 400 to 900 °C for 2 h to complete the crystallization process.

2.2. Characterization

The powders were analyzed by several techniques. The thermal decomposition of the α-BZN precursor was examined by differential scanning calorimetry (TG/DSC) (NETZSCH, STA404) at a heating rate of 10 °C min^{-1} under air flux. The crystalline phases were determined by X-ray diffraction (DRX) using an INEL curved position-sensitive detector operating with Cu$K\alpha$ radiation. The particle size was determined from the surface area values measured by N_2 adsorption/desorption isotherms BET (MICROMERITICS 2000), from a sample treated at 700 °C for 2 h. The Fourier-transformed infrared (FTIR) spectra in the 400–4000 cm^{-1} range were recorded with a spectrometer (BOMEN-HARTMAN & BRAUN MB102) in the transmission mode (KBr method) with a resolution of 4 cm^{-1}. Raman spectra in the range of 100–1000 nm were obtained with a BRUKER spectrometer (FRA-106/S), using the 1064-nm excitation line of an Nd–YAG Laser. The data were recorded with the power at 60 mW, 100 scans and 4 cm^{-1} resolution. In addition, the diffuse reflectance spectra (DRS) were recorded between 300 and 800 nm using a UV-Vis spectrometer VARIAN (Cary 5). Scanning electron microscopy (SEM) (JEOL 6400) was used to examine the morphology of the powders treated at different temperatures.

3. Results and discussion

The 4 h thermal treatment of the resin at 300 °C resulted in a soft black powder, portions of which were heat-treated for 2 h at temperatures ranging from 400 to 900 °C.

Fig. 1 shows the TG–DSC curves of the BZN powder treated at 400 °C for 2 h. The DSC result reveals an exothermic peak centered at 500 °C, which is accompanied by a weight loss of organic material, and a small peak centered at 580 °C, which may correspond to the crystallization of the cubic phase. The total weight loss was around 65%; no weight loss occurred above 750 °C.

The evolution of the crystalline phase of the α-BZN pyrochlore was monitored by XRD, as shown in Fig. 2a. The presence of Bi_2O_3 phase (JCPDS 27-0050) was observed at 400 °C. At 500 °C, the pyrochlore phase was already formed and coexisted with the remaining Bi_2O_3 while, at 600 °C, the pyrochlore peaks were fairly broad, indicating small disordered crystallites. As expected, increasing the annealing temperature caused the degree of crystallinity in the samples to increase, as illustrated in Fig. 2b.

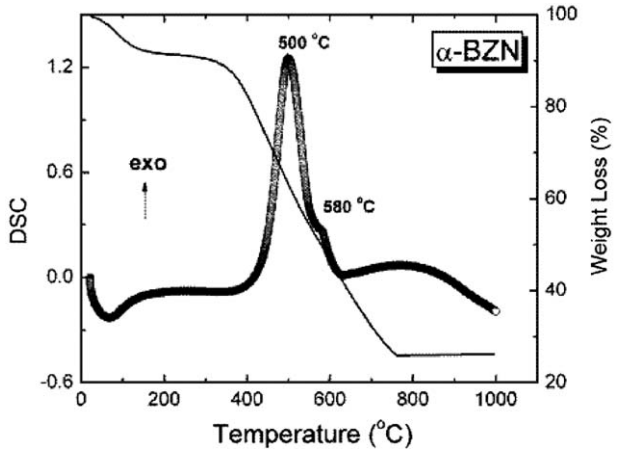

Fig. 1. Thermal analysis of the BZN powder treated at 400 °C for 4 h.

It is worth noting that reports of similar studies of BZN prepared by solid-state reaction state that the pyrochlore phase crystallizes through the formation of an intermediary $BiNbO_4$ phase. According to Nino et al. [4] and Wang et al. [6], at low temperatures Bi and Nb cations react to form the $BiNbO_4$ compound, while the formation of the pyrochlore phase occurs through the reaction of $BiNbO_4$ and ZnO. These authors also observed the formation of an intermediary orthorhombic pyrochlore phase which reacted with ZnO and transformed into cubic pyrochlore at temperatures above 750 °C. Chen et al. [5] studied the chemical reactions occurring in the formation of cubic-BZN and reported that the intermediate Bi–Nb–O oxides dominated the phase formation. They observed that cubic-BZN could be formed through the reaction of $BiNbO_4$ intermediate phase with ZnO at temperatures above 800 °C.

For the sake of comparison, Fig. 2c shows the X-ray patterns of the $BiNbO_4$ and orthorhombic BZN pyrochlore ($Bi_2(Zn_{1/3}Nb_{2/3})_2O_7$), both synthesized by the same procedure and treated at 700 °C for 2 h. At this temperature, the $BiNbO_4$ powder presented a mixture of $BiNbO_4$ (JCPDS 16-0486) and $Bi_5Nb_3O_{15}$ (JCPDS 16-0293) phases.

As can be seen, at a temperature as low as 500 °C, the cubic pyrochlore phase was already present, coexisting with a second phase which was probably some remanent Bi_2O_3 (indicated by the deconvolution of the peak with 2θ between 28° and 31°). At 600 °C, the sample was transformed into a cubic-BZN single-phased powder.

In this study, no detectable intermediary phases such as $BiNbO_4$ or $Bi_5Nb_3O_{15}$ or a pseudo-orthorhombic pyrochlore phase were observed at any time in the cubic-BZN composition (Fig. 2b), indicating that the chemical synthesis conferred a higher chemical homogeneity and reactivity on the powder, modifying the crystallization mechanism of the pyrochlore phase.

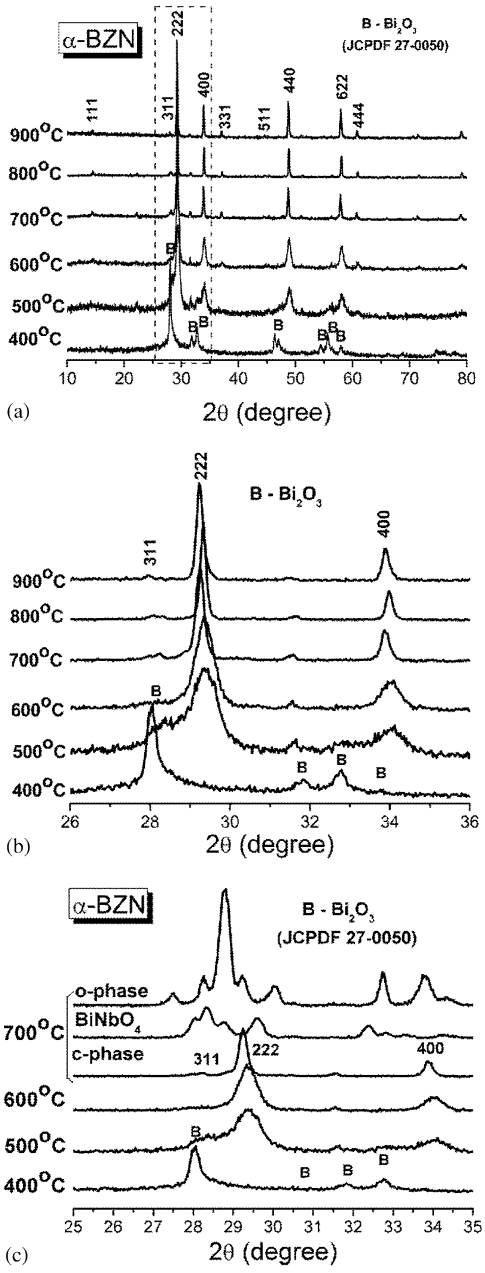

Fig. 2. XRD results for α-BZN powders treated at different temperatures: (a) Extended 2θ range; (b) Zoomed 2θ range (25–35°); (c) Zoomed 2θ range (25–35°) including $BiNbO_4$ and orthorhombic-BZN powders.

Fig. 3 shows the FT-IR spectra for the powders heated from 400 to 900 °C. All the spectra display bands characteristic of O–H stretching modes (3437 and 1640 cm^{-1}) and CH stretching modes (2920 cm^{-1}), and several bands characteristic of the oxygen-metals/ stretching mode at around 600 and 500 cm^{-1}. The powder treated at 400 °C also revealed bands at 1498, 1380 and 1280 cm^{-1} (carboxyl group stretching modes), and the band at around 1640 cm^{-1} (OH stretching mode) was shifted to 1609 cm^{-1}. Heat treatment at

higher temperatures led to a significant change in the infrared spectra, causing the bands at 1498 and 1280 cm^{-1} to disappear. At 900 °C, the band at about 600 cm^{-1} was associated with the B–O stretching vibration in the BO_6 octahedron, while the band at about 500 cm^{-1} was related to the *A*–O′ stretching vibration [13,14].

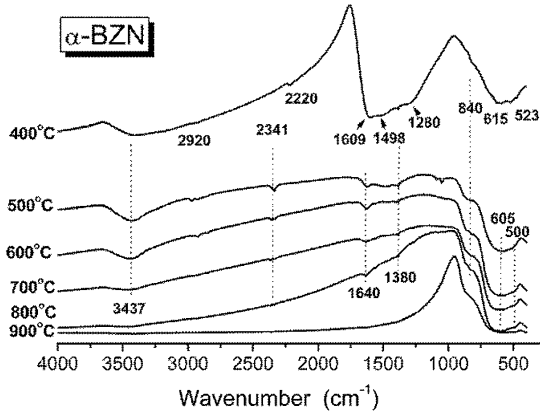

Fig. 3. FT-IR spectra for the α-BZN powders heated at temperatures from 400 to 900 °C.

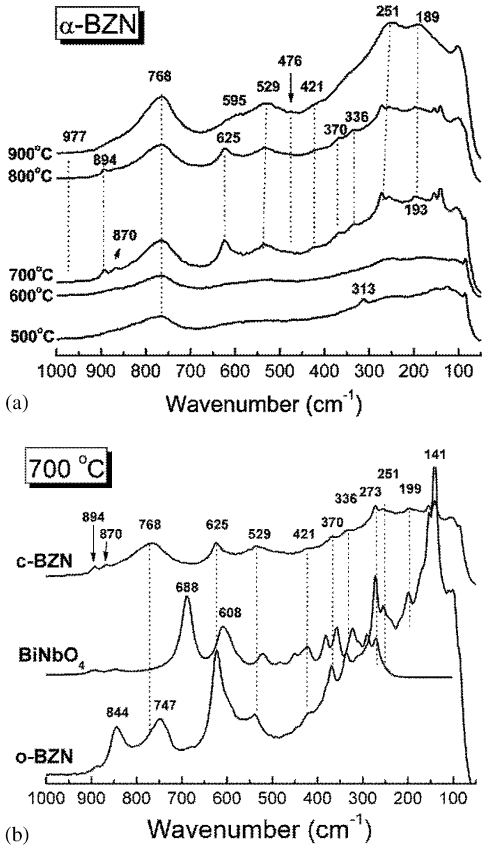

Fig. 4. Raman spectra of: (a) α-BZN powders treated at different temperatures—500 °C, 600 °C, 700 °C, 800 °C, 900 °C; (b) cubic-BZN, $BiNbO_4$ and orthorhombic-BZN powders treated at 700 °C for 2 h.

Reports in the literature [7] state that the Raman spectrum of BZN pyrochlore shows the followings bands: 189, 251, 421, 370, 529, 625, 768, and 977 cm^{-1}. Fig. 4 displays the Raman spectra of powders treated at temperatures ranging from 500 to 900 °C. The broadness of the features, probably due to the nanometric particles, prevents an accurate estimation of the precise band frequencies. It can be observed that the spectra underwent some modifications as the temperature rose. At 500 and 600 °C, the strongest band observed (768 cm^{-1}) was the one related with the Nb–O bond. At 700 °C, the bands related to the Bi–O (189 cm^{-1}) and Zn–O (251 cm^{-1}) bonds appeared slightly shifted due to the disordered structure, and several new vibrational modes appeared.

The bands located at 189, 251, 529, 595, 768 and 977 cm^{-1} were observed in the powder treated at 900 °C. The bands at 977 and 251 cm^{-1} were attributed to the Zn–O stretching modes, while those at 189 and 768 cm^{-1} were attributed to the Bi–O and Nb–O stretching modes, respectively. The bands at 529 and 595 cm^{-1} were found to correspond to the O–B–O bond bend. When the temperature of the thermal treatment rose to 900 °C, the bands at 336, 370, 421, 625, and 894 cm^{-1} disappeared. The aforementioned authors [7], stated that the movable Zn^{+2} is inclined to occupy the *B* site

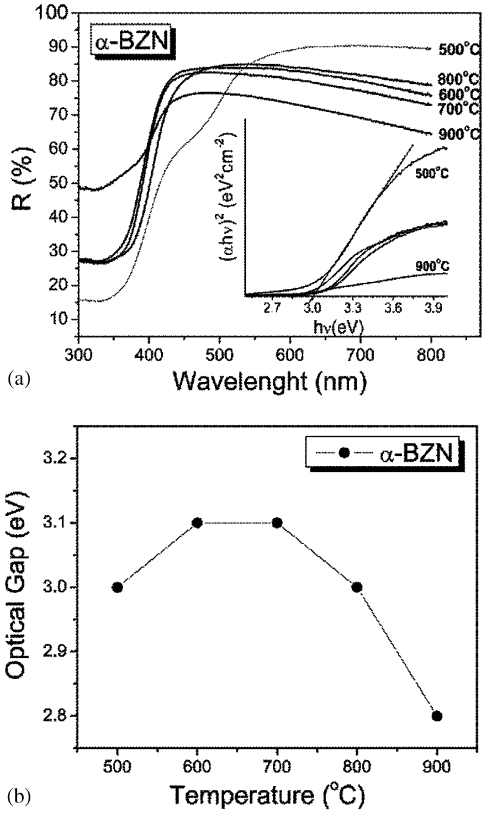

Fig. 5. (a) Diffuse reflectance of the powders treated at temperatures from 500 to 900 °C; (b) Optical gap as a function of the temperature for powders treated from 500 to 900 °C.

first, entering the *A* site only after the *B* site is fully occupied. Thus, it is reasonable to assume that some of these bands may relate to Zn–O bonds in the *A* site, which was partially occupied in the samples treated at 700 and 800 °C, causing locally disordered structures. Although the samples treated at 700, 800, and 900 °C showed the same XRD results, indicating the same long distance arrangement, the Raman spectra indicated a high level of localized short-range disorder observed for the lower temperature treatments. The Raman spectra of samples treated at 600 and 500 °C differed considerably from those obtained at 900, 800, and 700 °C.

The Raman results also confirmed the powder's single-phase nature observed by XRD even when treated at a low temperature (700 °C). Except for the band at around 625 cm^{-1}, no bands were observed at 844, 747 and 688 cm^{-1}, which relate to the main bands of $BiNbO_4$ and orthorhombic-BZN phases, as shown in Fig. 4b.

Fig. 5a shows the evolution of the diffuse reflectance spectra of five representative powders heat-treated at different temperatures. The absorbance values were calculated from the reflectance data, and the inset shows a plot of $(h\alpha\nu)^2$ against $h\nu$, from which the direct allowed band gap was estimated [15]. The optical band gaps obtained from these spectra are displayed in Fig. 5b. At temperatures varying from 500 to 700 °C, the band gap values were around 3.0–3.1 eV, indicating that the pyrochlore phase was already crystallized at 500 °C, according to the XRD data. The band gap values declined slightly to 3.0–2.8 eV in the powders treated at 800 and 900 °C, respectively. The difference in the band gap values may have been due to structural rearrangements, in accordance with the Raman spectra. However, DRS spectra are known to be sensitive to particle size [15]. Since a drastic change in particle growth was observed at higher temperatures, as indicated by SEM (shown in Fig. 6), the difference in the microstructure possibly explains the lower band gap value as the temperature rose to 900 °C.

The evolution of particle growth in the powders treated at different temperatures, as observed by SEM, is shown below (Fig. 6). The images clearly reveal an extraordinary variation of particle growth with thermal treatment. Samples prepared at 700 °C (Fig. 6a) were composed of large agglomerated clusters with dimensions of hundreds of nanometers, while annealing at 800 °C led to the formation of larger particles (Fig. 6b). Lastly, the thermal treatment at 900 °C gave rise to homogeneous sintered clusters with sizes exceeding 1 μm (Fig. 6c). It is worth mentioning that the particle size of the powder treated at 700 °C, calculated from the

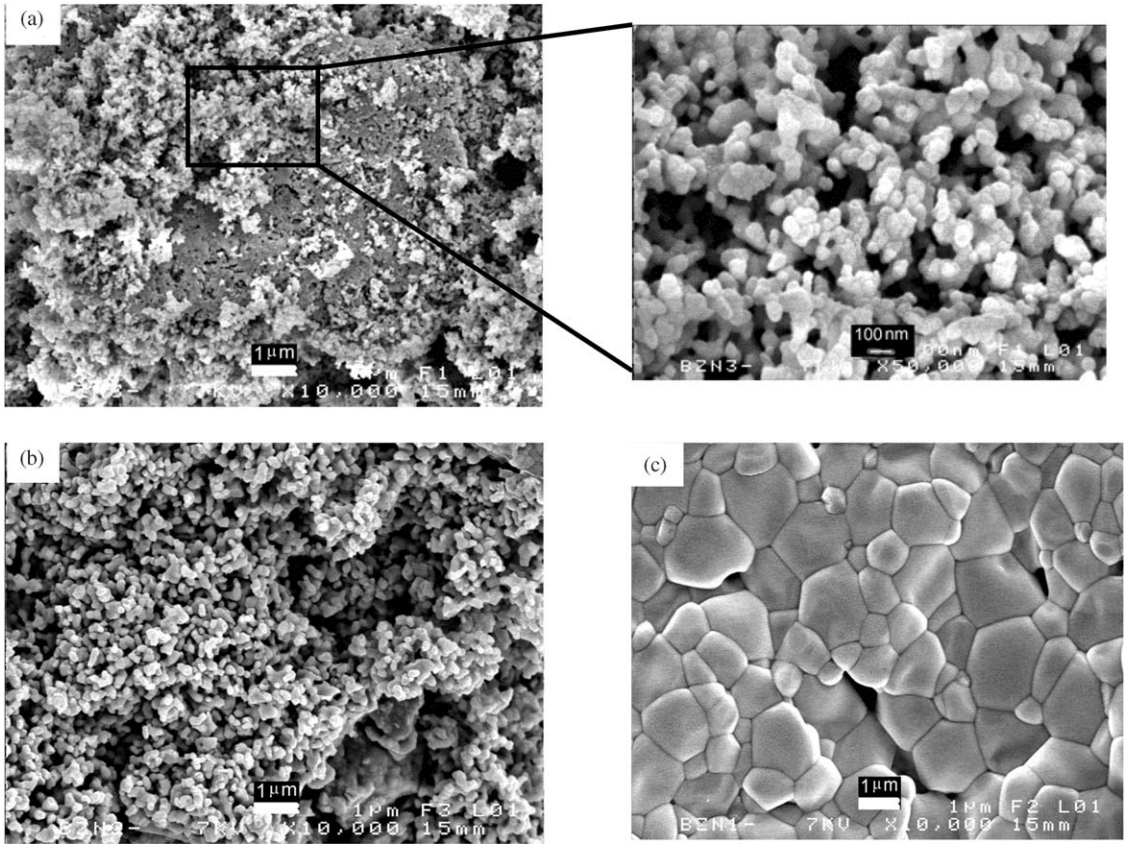

Fig. 6. SEM images of powders treated for 2 h at: (a) 700 °C, (b) 800 °C, (c) 900 °C.

surface area ($7.8\,m^2\,g^{-1}$) measured by N_2 adsorption/desorption isotherms (BET), was 108 nm, which represents a tenfold growth in particle size.

4. Conclusions

Cubic bismuth zinc niobate pyrochlore (α-BZN) was synthesized by the chemical route based on the polymeric precursor method. The study of phase formation revealed that a well-crystallized single-phased nanopowder was obtained after calcination at 700 °C. No $BiNbO_4$ or pseudo-orthorhombic intermediary phase was observed and the cubic pyrochlore phase was already formed after thermal treatment at temperatures as low as 500 °C. The Raman spectra revealed that, although the samples treated at 700, 800, and 900 °C showed the same XRD results, a high level of localized short-range disorder is observed for lower temperature treatments. The optical band gap for the powders treated between 500 and 700 °C, calculated from diffuse reflectance spectra, was 3.0–3.1 eV, indicating the low temperature crystallization of the pyrochlore phase. The low crystallization temperature and the phase purity of the powder were attributed to the material's high chemical homogeneity and reactivity achieved by the chemical route.

Acknowledgements

The work was supported by the Brazilian financing agency FAPESP. The authors would like to thank LCSIM–Université de Rennes I—France, for the XRD and SEM facilities, and LIEC–UFSCar–Brazil, for the Raman and UV-Vis diffuse reflectance measurements.

References

[1] I. Levin, T.G. Amos, J.C. Nino, et al., J. Solid State Chem. 168 (2002) 69–75.
[2] M. Valant, P.K. Davies, J. Mater. Sci. 34 (1999) 5437–5442.
[3] D.H. Liu, Y. Liu, S.Q. Huang, X. Yao, J. Am. Ceramic Soc. 76 (1993) 2129–2132.
[4] J.C. Nino, M.T. Lanagan, C.A. Randall, J. Mater. Res. 16 (2001) 1460–1464.
[5] S.Y. Chen, S.Y. Lee, Y.J. Lin, J. Eur. Ceramic Soc. 23 (2003) 873–881.
[6] X.L. Wang, H. Wang, X. Yao, J. Am. Ceramic Soc. 80 (1997) 2745–2748.
[7] H. Wang, H. Du, X. Yao, Mater. Sci. Eng. B 99 (2003) 20–24.
[8] M. Pechini, US Patent No. 3.330.697, 1967.
[9] S.M. Zanetti, E.R. Leite, E. Longo, J.A. Varela, J. Eur. Ceramic Soc. 19 (1999) 1409–1412.
[10] S.M. Zanetti, E.R. Leite, E. Longo, et al., J. Mater. Res. 15 (2000) 2091–2095.
[11] E.C. Paris, E.R. Leite, E. Longo, J.A. Varela, Mater. Lett. 37 (1998) 1–5.
[12] A.Z. Simões, A.M.H. Gonzalez, A.C. Cavalheiro, et al., Key Eng. Mater. 206 (2002) 1477–1480.
[13] H. Du, X. Yao, L. Zhang, Ceram. Int. 28 (2002) 231–348.
[14] J.C. Nino, M.T. Lanagan, C.A. Randall, S. Kamba, Appl. Phys. Lett. 81 (2002) 4404–4406.
[15] B.M. Weckhuysen, R.A. Schoonheydt, Catal. Today 49 (1999) 441–451.